Chinese Journal of Physics 56 (2018) 1772–1780

Contents lists available at ScienceDirect

Chinese Journal of Physics

journal homepage: www.elsevier.com/locate/cjph

# An examination of the structural, electronic, elastic, vibrational and thermodynamic properties of $Ru_2YGa$ (Y = Sc, Ti and V) Heusler alloys

A. Candan[a,*], S. Akbudak[b], M. Özduran[c], A. İyigör[d]

[a] Department of Machinery and Metal Technology, Ahi Evran University, Kırşehir 40100, Turkey
[b] Department of Physics, Faculty of Arts and Sciences, Adıyaman University, Adıyaman 02100, Turkey
[c] Department of Physics, Faculty of Arts and Sciences, Ahi Evran University, Kırşehir 40100, Turkey
[d] Central Research and Practice Laboratory (AHİLAB), Ahi Evran University, Kırşehir 40100, Turkey

ARTICLE INFO

*Pacs:*
62.20.de
71.15.Mb
63.20.D-
65
71.20.-b

*Keywords:*
Elastic moduli
DFT
Phonon dispersion
Thermodynamic properties
Band structure

ABSTRACT

The structural, electronic, elastic, vibrational and thermodynamic properties of the $Ru_2YGa$ (Y = Sc, Ti and V) Heusler alloys in $L2_1$ type cubic structure have been analyzed systematically using first principles density functional theory (DFT) together with the Generalized Gradient Approximation (GGA) method. The values of calculated lattice constant ($a_0$), elastic constants ($Cij$), Bulk modulus ($B$), Shear modulus ($G$), ratios of $B/G$, Young's modulus ($E$) and Poisson ratio ($\nu$) are in good agreement with the available theoretical and experimental results. The electronic band structures, corresponding total and partial density of states have also been obtained. The calculated band structures demonstrate that Ru2YGa (Y = Sc, Ti and V) alloys are metallic. The phonon dispersion curves, total and partial density of states of these alloys have been computed for the first time by adopting the direct method. It is considered that all alloys are dynamically stable in $L2_1$ structure.

## 1. Introduction

Heusler alloys were first synthesized by German chemist Friedrich Heusler in 1903 by adding 3rd group elements to CuMn alloys [1]. First studied Heusler alloy was $Cu_2MnSn$. In this first Heusler alloy, instead of Sn atom, III-V group elements such as Al, As, Sb, Bi and B were used and similarly instead of Cu atom different transition metals were used. One of the main characteristics of Heusler alloys is that although elements forming Heusler alloy are not ferromagnetic, some Heusler alloys show ferromagnetic behavior. Heusler alloys can be divided into two main categories such as full Heusler alloys and semi-Heusler alloys. Full-Heusler alloys are in $X_2YZ$ stoichiometric composition and have $L2_1$ body-centered cubic structure whereas Semi-Hesuler alloys are in XYZ stoichiometric composition and have $C1_b$ cubic-centered structure.

In Full Heusler alloys X is usually a transition metal, such as Cu, Fe, Ni, Co, Ru; Y is usually Mn, Cr or V and $Z$ can be Al, Ga, Ge, Si, Sn in $L2_1$ structure. Full Heusler alloys are triple intermetallic compounds and have cubic structure [2–5]. Intermetallic alloys, crystal structured compounds or solid solutions formed in the frame of basic proportions by two pure metals which take place between metals and ceramics usually have no resemblance to each other chemically. Intermetallic alloys which are a metal attached material class at critical temperature range ($T_c$ < 700 °C) forming regular crystal structures at long distance show metallic character. Most of the Heusler type alloys are ferromagnetic and show interesting ferromagnetic characteristics [6,7]. These alloys have the ability to

* Corresponding author.
*E-mail address:* acandan@ahievran.edu.tr (A. Candan).

https://doi.org/10.1016/j.cjph.2018.05.006
Received 31 January 2018; Received in revised form 4 April 2018; Accepted 4 May 2018
Available online 28 May 2018

show a violant magnetization in the exististence of a weak magnetic field. In case of removal or ceasing of the magnetic field, these alloys still show magnetism which is called remanence. Magnetic remanence value determines the permanent magnetism state. Heusler type alloys, constructed gathering of the elements has changeable magnetism which is a unique characteristics of these alloys [8]. Another important characteristics of Heusler alloys is that they can have magnetic shaped memory [9,10]. Shaped memory alloys have the ability to return to their original size or form in proper thermal and mechanical processes after their geometry is disrupted due to external factors. Because of their interesting half-metallic properties, Heusler alloys are used in many technological areas such as spintronics and magnetoelectronics [11,12]. The main characteristic of half-metallic ferromagnets is their different behavior in the two spin bands: while the majority spin band shows a typical metallic behavior, the minority spin band is semiconducting. Thus, the spin polarization at the Fermi level is 100%, that maximizes the efficiency of spintronic devices [13]. Recently, these alloys have attracted considerable interest because of their interesting magnetic properties [14–19]. Magnetic susceptibility and permeability, magnetostriction, Curie temperature and hysteresis curves studies of the Heusler alloys are fundamental topics [20,21]. $Ru_2YGa$ (Y = Sc, Ti, and V) have been subject of various theoretical and experimental studies [22–26]. Theoretically, using the full-potential linearized augmented plane-wave (FP-LAPW) method based on the density functional theory (DFT), Abbassa et al. [22] reported the structural, electronic, elastic and thermal properties for $Ru_2VGa_{1-x}Al_x$ (x = 0, 0.25, 0.5, 0.75, 1). Gilleßen in his dissertation studied the lattice constants and magnetic moments of full Heusler alloys $Ru_2YGa$ (Y = Sc, Ti, and V) using density functional theory [26]. On the experimental side, $Ru_2VGa$ alloy has been synthesized for the first time by Mondal et al. [23]. The lattice constant and electrical resistivity of the $Ru_2VGa$ alloy has been calculated using powder X-ray powder diffraction (XRD) by Mondal et al. [24]. They state that the $Ru_2VGa$ alloy shows high resistances compared to standard metals and have low residual resistivity ratio.

In the present paper we have carried out first principles density functional theory calculations at PBE level of theory to obtain physical parameters such as lattice constant ($a_0$), elastic constants ($C_{ij}$), Bulk modulus ($B$), Shear modulus ($G$), ratio of $B/G$, Young's modulus ($E$) and Poisson ratio ($\nu$) of $Ru_2YGa$ (Y = Sc, Ti, and V) Heusler alloys. We have also calculated electronic band structures, corresponding total and partial density of states (PDOS), phonon dispersion relations and thermodynamic properties such as specific heat ($C_v$) and entropy ($S$) of these Heusler alloys.

Organization of this paper is as follows: We describe the theoretical method in Section 2. Results and discussions are given in Section 3. Finally, results are recapitulated in Section 4.

## 2. Theoretical method

All the calculations have been performed using the plane-wave pseudo-potential DFT method implemented in the MedeA-VASP package [27,28]. Projector Augmented Wave (PAW) pseudo-potentials were used to present the ionic potentials. The Perdew–Burke–Ernzerhof (PBE) [29] exchange-correlation functional was treated at the Generalized Gradient Approximation (GGA). An energy cut-off 329 eV was found to be adequate for the calculation of the structural, electronic, elastic, vibrational and thermodynamic properties of $Ru_2VGa$. Similarly, an energy cut-off of 313 eV was found to be adequate for $Ru_2ScGa$ and $Ru_2TiGa$. The Brillouin zone integration was performed on a Monkhorst-Pack [30] 6 × 6 × 6 k-point mesh with a Methfessel–Paxton [31] smearing of 0.225 eV for $Ru_2VGa$ and $Ru_2ScGa$. For $Ru_2TiGa$ 5 × 5 × 5 k-point mesh with a smearing of 0.225 eV was used. The elastic constants were predicted using the stress-finite strain technique [32]. The phonon dispersion curves, total and PDOS of these alloys were calculated using the direct method [33].

## 3. Results and discussion

### 3.1. Structural and electronic properties

Heusler type alloys having X 2 YZ stoichiometric composition belongs to Fm-3 m (space group No. 225). This structure may conveniently be considered as four interpenetrating fcc sublattices with atoms of X, Y and Z at locations (0, 0, 0) and (1/2, 1/2, 1/2); (1/4, 1/4, 1/4); and (3/4, 3/4, 3/4), respectively [5,17]. The crystal structure of $Ru_2YGa$ (Y = Sc, Ti, and V) Heusler alloys is given in Fig. 1. Additionally, the calculated lattice constants ($a_0$) are listed in Table 1. The optimized lattice constants of $Ru_2ScGa$, $Ru_2TiGa$, and $Ru_2VGa$ are 6.229, 6.098, and 6.013 Å, respectively. It is known that ionic radius of Sc, Ti and V atoms decrease from Sc to V. Lattice constants of $Ru_2YGa$ (Y = Sc, Ti, and V) Heusler alloys increase while ionic radius of the Y atom increases as shown in Table 1. The obtained results for $Ru_2YGa$ (Y = Sc, Ti, and V) alloys agree well with the available experimental and theoretical results in the literature [22–26]. Therefore, there is a good agreement between our results and previously reported results.

The calculated electronic band structure, relevant total and partial DOS of $Ru_2ScGa$, $Ru_2TiGa$ and $Ru_2VGa$ along the high symmetry directions in the Brillouin zone are given in Figs. 2 and 3. It is seen that there is no band gap at the Fermi level, as a result, $Ru_2ScGa$, $Ru_2TiGa$ and $Ru_2VGa$ alloys exhibit a metallic behavior. Our calculated electronic band structure for $Ru_2VGa$ is in good agreement with previous reported work [22].

From total and partial density of states relations of $Ru_2ScGa$ alloy as shown in Fig. 3, the most contribution to conductivity comes from Ru-4d and Ga-4 s orbitals between −6.4 eV and −8.5 eV and similarly from Ru-4d and Ga-4 s orbitals between −4.5 eV and 0 eV (Fermi level). It is clearly seen that sharp peaks over Fermi level having energies of 2.2 eV and 3.7 eV are provided by the electrons in Ru-4d and Sc-3d.

From total and partial density of states relations of $Ru_2TiGa$ alloy as shown in Fig. 3, the most contribution to conductivity comes from the electrons in Ru-4d and Ga-4 s orbitals between −6.5 eV and −8.7 eV and from the electrons in Ru-4d and Ti-3d orbitals between −5.0 eV and Fermi level. It is clearly seen that sharp peaks over Fermi level having energies of 2.2 eV are provided by the

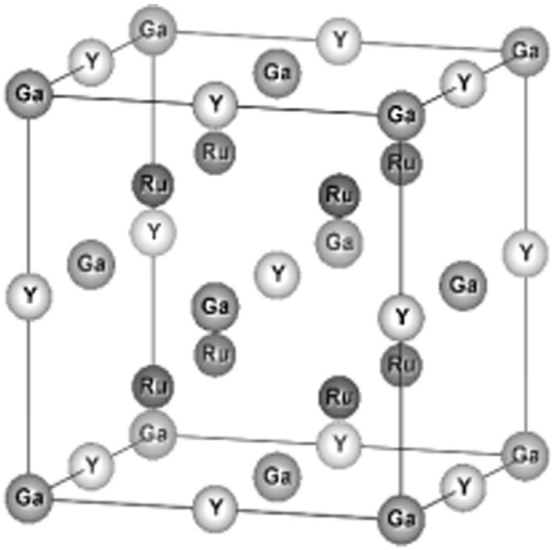


**Fig. 1.** Crystal structure of Heusler alloys $Ru_2YGa$ (Y = Sc, Ti and V).

**Table 1**
Calculated lattice constant ($a_0$), elastic constants ($C_{ij}$), Bulk modulus ($B$), Shear modulus ($G$), ratio of $B/G$, Young's modulus ($E$), Poisson ratio ($\nu$) and hardness ($H_v$) of $Ru_2YGa$ (Y = Sc, Ti and V) alloys.

| Compounds | References | $a_0$ (Å) | $C_{11}$ (GPa) | $C_{12}$ (GPa) | $C_{44}$ (GPa) | $B$ (GPa) | $G$ (GPa) | $B/G$ | $E$ (GPa) | $\nu$ | $H_v$ (GPa) |
|---|---|---|---|---|---|---|---|---|---|---|---|
| $Ru_2ScGa$ | Present | 6.229 | 236.11 | 126.95 | 79.93 | 163.34 | 68.59 | 2.38 | 180.52 | 0.315 | 5.59 |
| | [26] | 6.225 | – | – | – | – | – | – | – | – | – |
| $Ru_2TiGa$ | Present | 6.098 | 303.29 | 164.70 | 103.70 | 210.89 | 88.23 | 2.39 | 232.29 | 0.316 | 6.91 |
| | [26] | 6.100 | – | – | – | – | – | – | – | – | – |
| $Ru_2VGa$ | Present | 6.013 | 385.76 | 160.67 | 113.86 | 235.70 | 113.33 | 2.08 | 293.03 | 0.293 | 10.51 |
| | [22] | 6.032 | 388.01 | 168.10 | 107.95 | 241.40 | 108.75 | 2.22 | 283.65 | 0.30 | – |
| | [23, 24-Exp.] | 5.994 | – | – | – | – | – | – | – | – | – |
| | [25-Exp.] | 5.989 | – | – | – | – | – | – | – | – | – |
| | [26] | 6.015 | – | – | – | – | – | – | – | – | – |

electrons in Ru-4d and Ti-3d.

From the total and the partial density of states of $Ru_2VGa$ as shown in Fig. 3, the low-energy part between −7 eV and −9.8 eV density of states are mainly consisted by Ru-4d states and Ga-4s states for $Ru_2VGa$. The predominant contributions of the density of states between −6 eV and Fermi level mainly come from the Ru-4d and V-3d states for $Ru_2VGa$. Similarly, the contribution of one peak, around 1 eV above the Fermi level, is dominated by Ru-4d states and V-3d states for $Ru_2VGa$. Our calculated total and the PDOS for $Ru_2VGa$ are in good agreement with the available theoretical result [22].

### 3.2. Elastic properties

Elastic constants are significant parameters of a material and often provide valuable information on the mechanical stability. The calculated Bulk modulus ($B$), elastic constants ($C_{ij}$), Shear modulus ($G$), Young's modulus ($E$), Poisson ratio ($\nu$) and hardness ($H_v$) of $Ru_2YGa$ (Y = Sc, Ti, and V) Heusler alloys are given in Table 1. Value of calculated Bulk modulus (235.70 GPa) for $Ru_2VGa$ is smaller than the value calculated using FPLAPW method (241.40 GPa) [22]. When Bulk modulus of these alloys are compared, it is seen that there is a following relation; $Ru_2ScGa < Ru_2TiGa < Ru_2VGa$ that is to say Bulk modulus decreases as ionic radius of Y atom increases which is clearly seen from Table 1. Young modulus ($E$) is a measure of the stiffness. As the value of $E$ increases, the stiffness of the material increases. Stiffness ordering based on the calculated Young modulus values for these alloys is given as $Ru_2VGa > Ru_2TiGa > Ru_2ScGa$.

A cubic system has three independent elastic constants ($C_{11}$, $C_{12}$, $C_{44}$). Mechanical stability of these alloys has been analyzed in terms of their elastic constants. For cubic crystals, the conditions for mechanical stability are given by [34]:

$$C_{11} > 0, \quad C_{44} > 0, \quad C_{11} + 2C_{12} > 0, \quad C_{11} - C_{12} > 0$$

The obtained elastic constants for $Ru_2YGa$ (Y = Sc, Ti, and V) satisfy these mechanical stability criterions, indicating that the $Ru_2YGa$ alloys are mechanically stable in the $L2_1$ structure.

After obtaining the required information about the elastic constants we can have a deep insight about the ductile and brittle

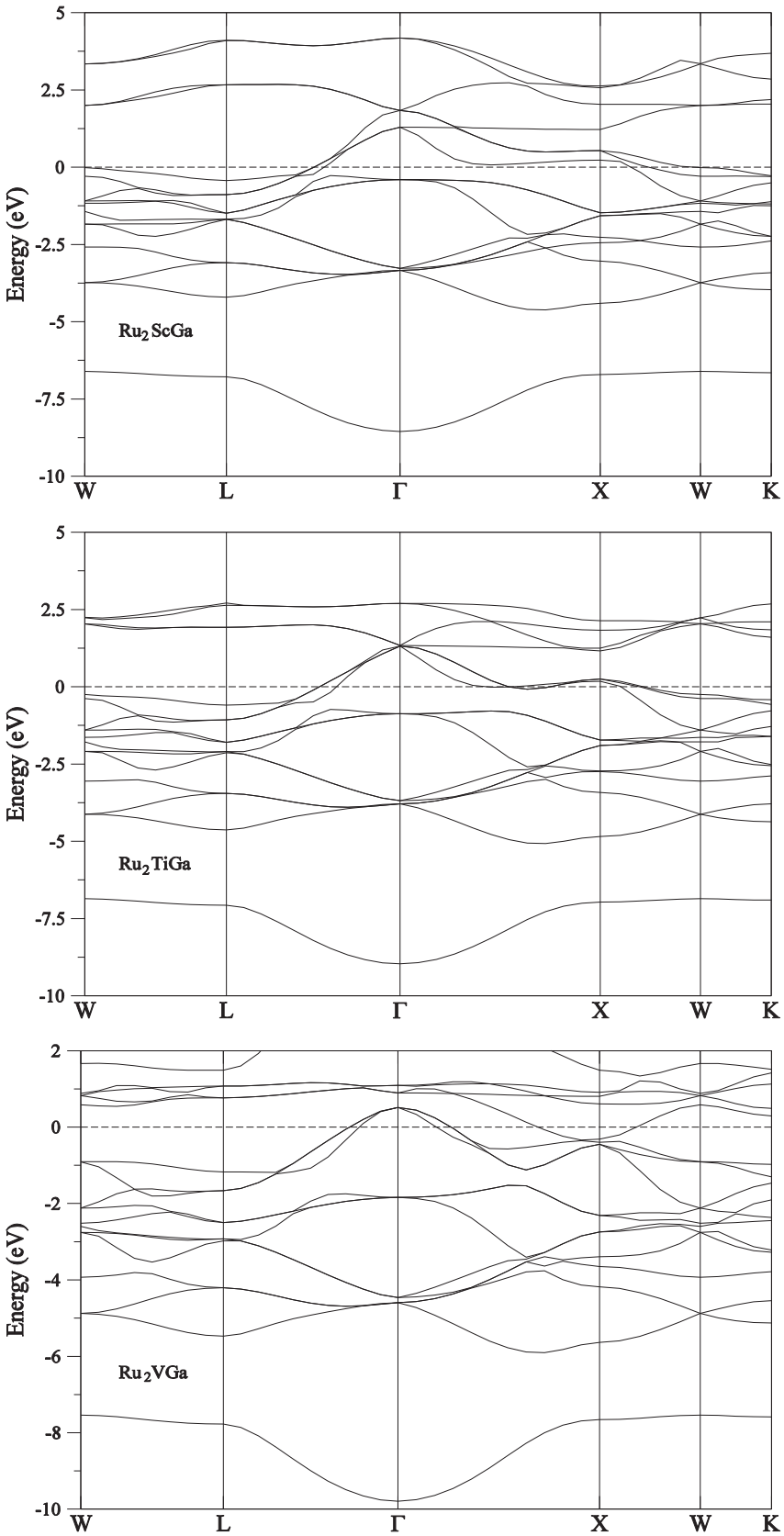


**Fig. 2.** The calculated electronic band structure for $Ru_2YGa$ (Y = Sc, Ti and V) along the high symmetry directions in the Brillouin zone.

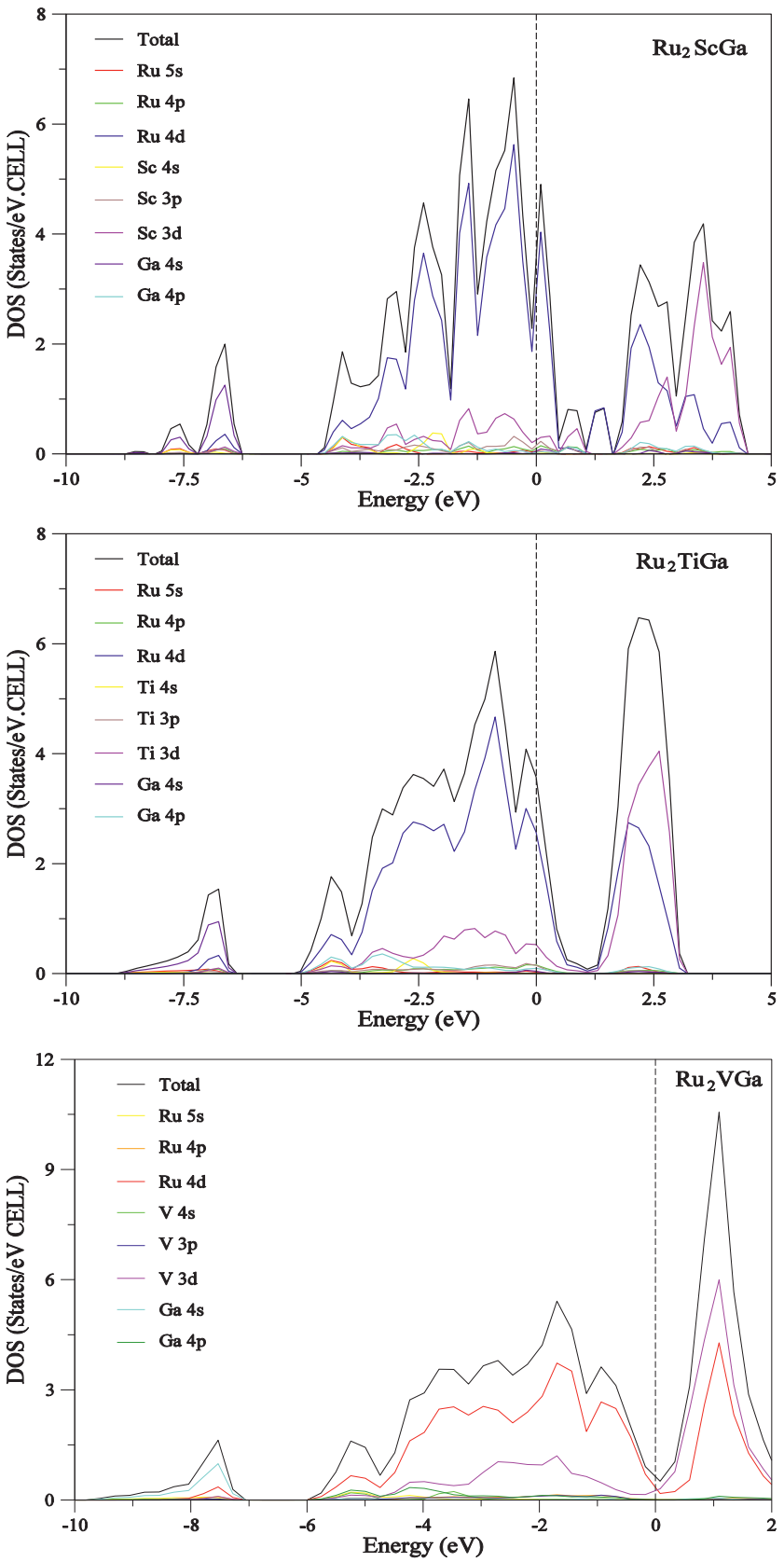


**Fig. 3.** Calculated total and partial density of states for $Ru_2YGa$ (Y = Sc, Ti and V) alloys.

nature of these alloys. There are several parameters such as Cauchy pressure ($C_{12}$–$C_{44}$), Pugh's index of ductility ($B/G$) and Poisson's ratio ($\nu$) that enable us to determine the ductile and brittle nature of the given material. Firstly, the Cauchy's pressure is defined as the difference between the elastic constants $C_{12}$ and $C_{44}$ ($C_{12}$–$C_{44}$) and is a measure of ductility [35–37]. As long as the Cauchy pressure is positive, the material is ductile. On the other hand, if it is negative, the material is expected to be brittle in nature. The value of the Cauchy's pressure is found to be 47.02 GPa for $Ru_2ScGa$, 61.00 GPa for $Ru_2TiGa$, and 46.81 GPa for $Ru_2VGa$, which obviously shows the ductile nature of these alloys.

Second index of ductility is the Pugh (B/G) ratio [38]. In order to investigate the ductility and brittleness properties of $Ru_2YGa$ (Y = Sc, Ti, V), the ratios of Bulk modulus to Shear modulus (B/G) have been calculated and results are listed in Table 1. If the ratio of B/G is higher than 1.75, then that material behaves in a ductile manner. If it is less than 1.75, then the material demonstrates brittleness [39,40]. The B/G values are 2.38, 2.39, and 2.08 for $Ru_2ScGa$, $Ru_2TiGa$, and $Ru_2VGa$, respectively. Therefore, $Ru_2YGa$ (Y = Sc, Ti, V) alloys can be classified as ductile materials. This is in good agreement with the results found for $Ru_2VGa$ [22]. Another parameter that determines the ductility and brittleness of the materials is Poisson's ratio ($\nu$) which was proposed by Frantsevich et al. [41]. According to Frantsevich rule, critical value that set aparts the ductile and brittle nature of the material is 0.26. For brittle materials, the Poisson's ratio is less than 0.26, otherwise it acts as ductile [42,43]. Here the calculated Poisson's ratios for $Ru_2YGa$ (Y = Sc, Ti, and V) are greater than critical value of 0.26 as seen in Table 1. Thus, these three alloys can be characterized as ductile material.

Finally, hardness value of $Ru_2YGa$ (Y = Sc, Ti, and V) alloys has been calculated by using the quasi-experimental approach which depends on Pugh's modulus ratio improved by Chen et al. [44] as given below;

$$H_V = 2(k^2G)^{0.585} - 3; \quad (k = G/B)$$

The calculated hardness values are given in Table 1. As shown in Table 1, $Ru_2VGa$ has the highest hardness value (10.51 GPa), while $Ru_2ScGa$ has the lowest (5.59 GPa).

### 3.3. Vibrational and thermodynamic properties

The phonon dispersion curves and relevant total and PDOS of $Ru_2YGa$ (Y = Sc, Ti, and V) Heusler alloys are shown in Fig. 4. Since there are four atoms in the primitive cell of $Ru_2YGa$ (Y = Sc, Ti, and V) Heusler alloys, there are twelve phonon modes for any wave vector. Three of these phonon modes are acoustic, and nine are optical modes. The calculated phonon dispersion curves of $Ru_2YGa$ (Y = Sc, Ti, and V) indicate that all alloys are stable dynamically in the $L2_1$ structure without any negative phonon frequencies. In Fig. 4, the computed optical frequency values are 2.637– 5.668– 7.524 for $Ru_2ScGa$, for $Ru_2TiGa$, 4.453– 6.004– 6.341 and for $Ru_2VGa$, 5.235– 6.779– 7.178, respectively. From the phonon dispersion, total and PDOS curves of $L2_1$ crystal structured $Ru_2ScGa$ Heusler alloy as shown in Fig. 4, it is clearly seen that there is a gap between optical-optical phonon modes of this alloy. This gap is due to the mass difference of Ru, Sc and Ga atoms. From total phonon density of states curve of $Ru_2ScGa$ Heusler alloy in Fig. 4, calculated gap is 1.27 THz. As we look to the PDOS curves we can see that for all alloys, all the atoms forming these alloys vibrates in acoustic and optical regions. Unfortunately, the experimental or theoretical phonon frequencies of $Ru_2YGa$ (Y = Sc, Ti, and V) alloys are not available in the literature for further comparison.

Specific heat-temperature relations for $Ru_2YGa$ (Y = Sc, Ti, and V) alloys are given in Fig. 5. As we look up Fig. 5; Though specific heat increases rapidly for $T \leq 200$ K it increases slowly for $T > 200$ K. Therefore, specific heat converges to a constant which is called as Dulong-Petit limit ($\sim 3NR$) at high temperatures [45]. Here $N$ is the number of atoms in unit cell and $R$ is ideal gas constant.

Fig. 6. shows the change of entropy as a function of temperature for $Ru_2YGa$ (Y = Sc, Ti, and V). As shown in Fig. 6 going from $Ru_2VGa$ to $Ru_2ScGa$ the entropy is increasing with temperature and this relation shows that as the ionic radius of Y (V, Ti and Sc) atom increases entropy also increases. As a consequence, we can infer that there is a direct relation between radius of Y atom and entropy.

## 4. Conclusions

In this paper, the structural, electronic, elastic, vibrational and thermodynamic properties for $Ru_2YGa$ (Y = Sc, Ti, and V) Heusler alloys have been investigated using density functional theory together with PBE exchange correlational functional. The computed lattice constant values are very close to the available results found in literature. Besides, obtained electronic band structure and their corresponding total and partial density of states show the metallic character of the $Ru_2YGa$ (Y = Sc, Ti, and V) Heusler alloys in the $L2_1$ phase. The calculated elastic constants have indicated that all the alloys are mechanically stable. The elastic properties like Bulk modulus, Shear modulus, Young's modulus, Pugh criterion, Poisson's ratio, Cauchy's pressure and hardness have also been calculated. The obtained results clearly display the ductile nature of the considered materials. Besides, $Ru_2VGa$ has the highest hardness whereas $Ru_2ScGa$ has the lowest. Phonon dispersion curves and their corresponding total and partial density of states for $Ru_2YGa$ (Y = Sc, Ti, and V) Heusler alloys have been computed for the first time using the MedeA-Phonon module with the help of the direct *ab-initio* force constant method. These alloys are dynamically stable in the L21 phase due to the fact that they do not have any negative phonon frequency. Furthermore, the relations of thermodynamic properties such as specific heat and entropy as a function of temperature have been acquired. The obtained results reveal that specific heat values converge to Dulong-Petit limit at high temperature. In the light of the above mentioned properties, Heusler alloys are very promising materials for different fields like shaped memory alloys and spintronics. Therefore, we believe that the results obtained in this paper will initiate new theoretical and experimental studies.

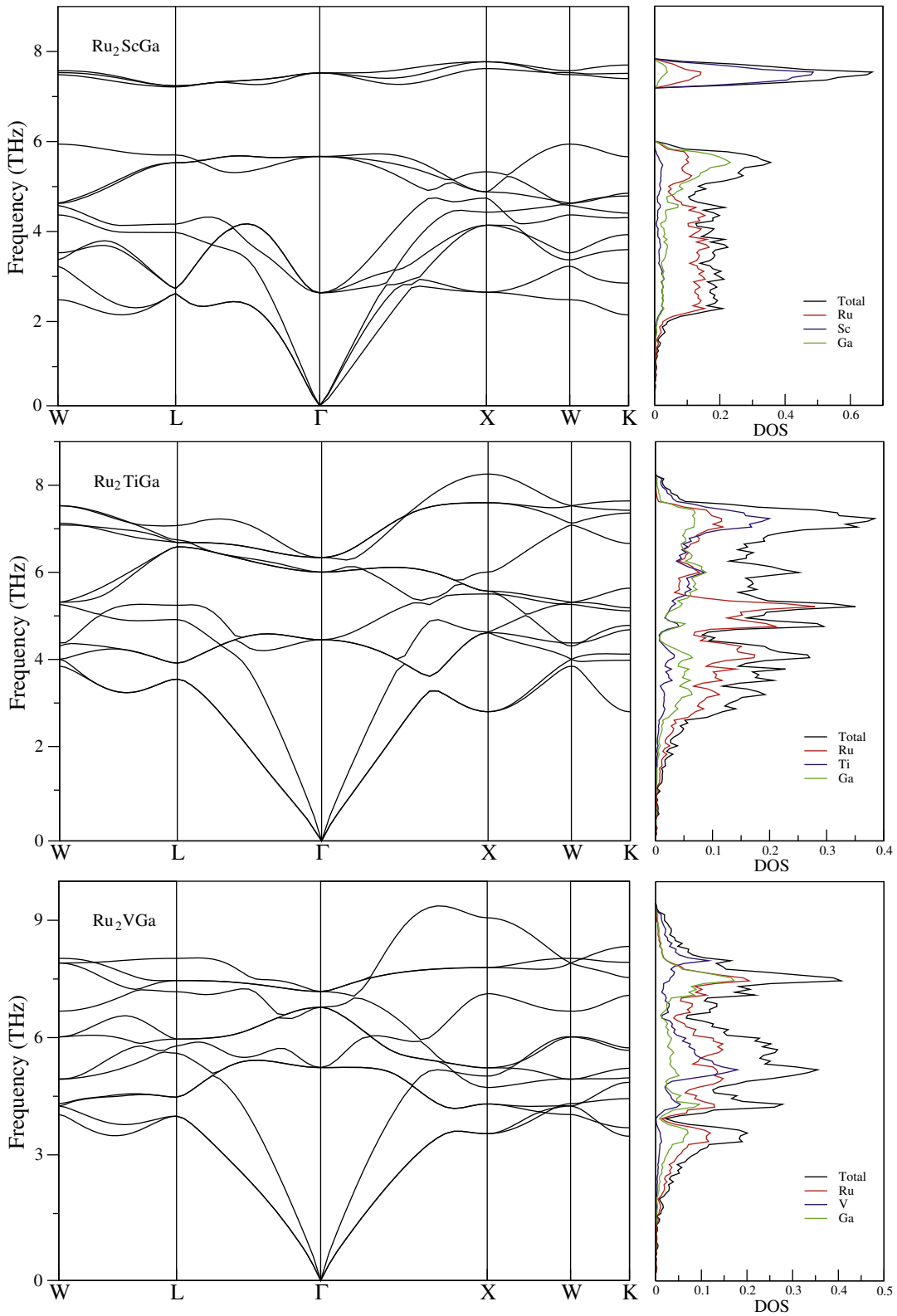


**Fig. 4.** Calculated phonon dispersion curves and phonon DOS for $Ru_2YGa$ (Y = Sc, Ti and V) alloys.

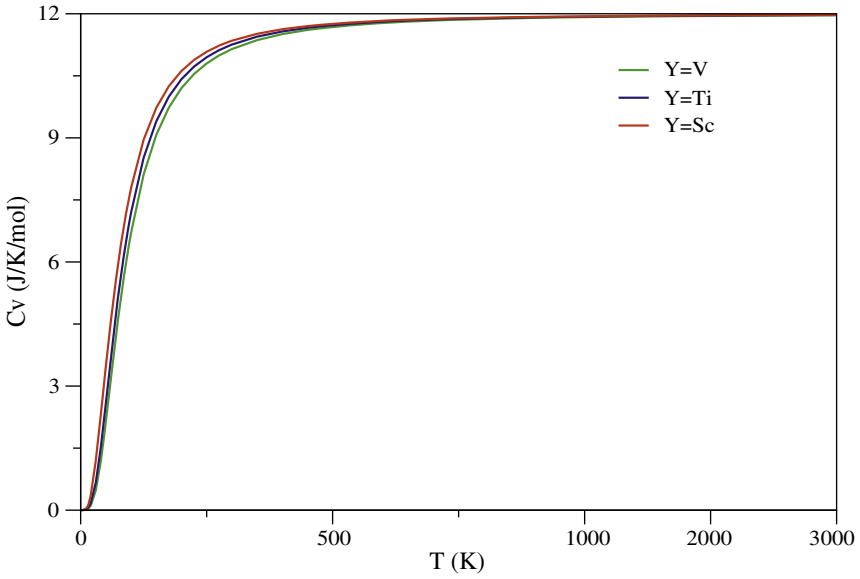


**Fig. 5.** The specific heats at constant pressure versus temperature for $Ru_2YGa$ (Y = Sc, Ti and V) alloys.

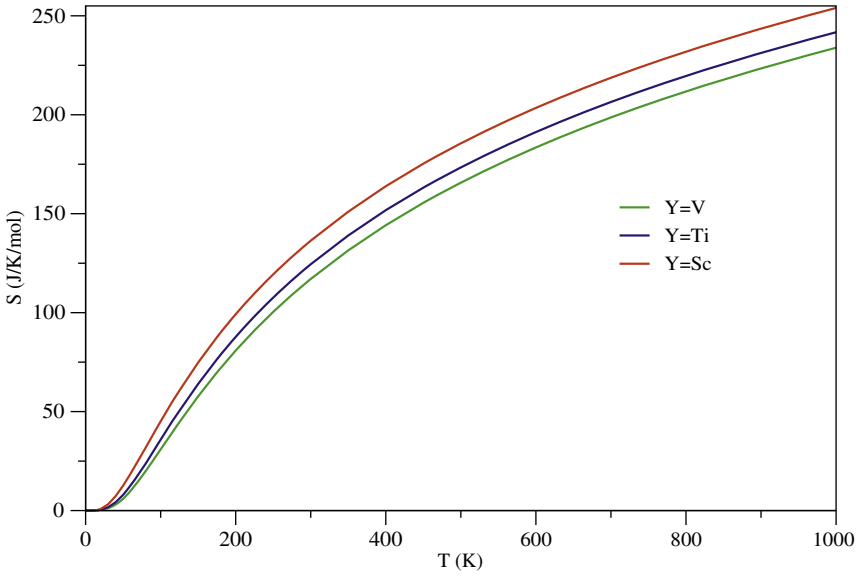


**Fig. 6.** The entropy versus temperature for $Ru_2YGa$ (Y = Sc, Ti and V) alloys.

## References

[1] F. Heusler, Verhandlugen Deutschen Physikalischen Gesellschaft 5 (1903) 219.
[2] S. Khmelevskyi, E. Simon, L. Szunyogh, P. Mohn, J. Alloys Compd. 692 (2017) 178–182.
[3] I. Galanakis, J. Phys. Condens. Matter 14 (2002) 6329–6340.
[4] S. Bosu, Y. Sakuraba, T.T. Sasaki, S. Li, and K. Hono, Scripta Materialia, Scr. Mater. 110 (2016) 70–73.
[5] A. Candan, G. Uğur, Z. Charifi, H. Baaziz, M.R. Ellialtıoğlu, J. Alloys Compd. 560 (2013) 215–222.
[6] S. Aksoy, T. Krenke, M. Acet, E.F. Wassermann, X. Moya, L. Mañosa, A. Planes, Appl. Phys. Lett. 91 (2007) 241916.
[7] X.Q. Chen, R. Podloucky, P. Rogl, J. Appl. Phys. 100 (2006) 113901.
[8] E. Şaşıoğlu, L.M. Sandratskii, P. Bruno, Phys. Rev. B 70 (2004) 024427.
[9] S. Aksoy, M. Acet, P.P. Deen, L. Mañosa, A. Planes, Phys. Rev. B 79 (2009) 212401.
[10] Z.H. Liu, M. Zhang, Y.T. Cui, Y.Q. Zhou, W.H. Wang, G.H. Wu, X.X. Zhang, G. Xiao, Appl. Phys. Lett. 82 (2003) 424–426.
[11] W. Wang, H. Sukegawa, R. Shan, T. Furubayashi, K. Inomata, Appl. Phys. Lett. 92 (2008) 221912.
[12] S.A. Wolf, D.D. Awschalom, R.A. Buhrman, J.M. Daughton, S. Von Molnár, M.L. Roukes, A.Y. Chtchelkanova, D.M. Treger, Science 294 (2001) 1488–1495.

[13] S. Fuji, S. Sugimurat, S. Ishida, S. Asano, J. Phys. Condens. Matter 2 (1990) 8583–8589.
[14] B. Saadi, Chin. J. Phys. 55 (2017) 195–202.
[15] I. Galanakis, P.H. Dederichs, N. Papanikolaou, Phys. Rev. B 66 (2002) 134428.
[16] S. Sonu, P. Kumar, Chin. J. Phys. 55 (2017) 1972–1980.
[17] I. Galanakis, P. Mavropoulos, P.H. Dederichs, J. Phys. D, 39 (2006) 765.
[18] F. Ahmadian, R. Alinajimi, Comput. Mater. Sci. 79 (2013) 345–351.
[19] S. Wurmehl, G.H. Fecher, H.C. Kandpal, V. Ksenofontov, C. Felser, H.J. Lin, J. Morais, Phys. Rev. B 72 (2005) 184434.
[20] J. Kübler, G.H. Fecher, C. Felser, Phys. Rev. B 76 (2007) 024414.
[21] N. Arıkan, A. İyigör, A. Candan, Ş. Uğur, Z. Charifi, H. Baaziz, G. Uğur, J. Mater. Sci. 49 (2014) 4180–4190.
[22] H. Abbassa, S. Hadjri-Mebarki, B. Amrani, T. Belaroussi, K.D. Khodja, P. Aubert, J. Alloys Compd. 637 (2015) 557–563.
[23] S. Mondal, C. Mazumdar, R. Ranganathan, American Institute of Physics Conference Series, vol. 1536, 2013, pp. 825–826.
[24] S. Mondal, C. Mazumdar, R. Ranganathan, American Institute of Physics Conference Series, vol. 1512, 2013, pp. 978–979.
[25] M. Yin, P. Nash, J. Alloys Compd. 634 (2015) 70–74.
[26] M. Gilleßen, R. Dronskowski, Maßgeschneidertes und Analytik-Ersatz: über die quantenchemischen Untersuchungen einiger ternärer intermetallischer Verbindungen (No. RWTH-CONV-113777), Fachgruppe Chemie (2010).
[27] G. Kresse, J. Hafner, Phys. Rev. B 47 (1993) 558.
[28] G. Kresse, J. Furthmuller, Phys. Rev. B 54 (1996) 11169.
[29] J.P. Perdew, K. Burke, M. Ernzerhof, Phys. Rev. Lett. 77 (1996) 3865.
[30] H.J. Monkhorst, J.D. Pack, Phys. Rev. B 13 (1976) 5188.
[31] M. Methfessel, A.T. Paxton, Phys. Rev. B 40 (1989) 3616.
[32] H. Nielsen, R.M. Martin, Phys. Rev. Lett. 50 (1983) 697.
[33] K. Parlinski, Z.Q. Li, Y. Kawazoe, Phys. Rev. Lett. 78 (1997) 4063.
[34] M. Born, K. Huang, Dynamical Theory of Crystal Lattices, (1954).
[35] M.H. Elahmar, H. Rached, D. Rached, R. Khenata, G. Murtaza, S.B. Omran, W.K. Ahmed, J. Magn. Magn. Mater. 393 (2015) 165–174.
[36] D.G. Pettifor, Mater. Sci. Technol. 8 (1992) 345–349.
[37] G. Vaitheeswaran, V. Kanchana, R.S. Kumar, A.L. Cornelius, M.F. Nicol, A. Svane, A. Delin, B. Johansson, Phys. Rev. B 76 (2007) 014107.
[38] S.F. Pugh, Philos. Mag. J. Sci. 45 (1954) 823–843.
[39] G. Surucu, Mater. Chem. Phys. 203 (2018) 106–117.
[40] G. Surucu, A. Erkisi, Mater. Res. Express 4 (2017) 106520.
[41] I.N. Frantsevich, F.F. Voronov, S.A. Bakuta, Elastic Constants and Elastic Moduli of Metals and Insulators Handbook, in: I.N. Frantsevich (Ed.), Naukova Dumka, Kiev, 1982, p. 60.
[42] M. Ahmad, G. Murtaza, R. Khenata, S.B. Omran, A. Bouhemadou, J. Magn. Magn. Mater. 377 (2015) 204–210.
[43] V. Kanchana, G. Vaitheeswaran, Y. Ma, Y. Xie, A. Svane, O. Eriksson, Phys. Rev. B 80 (2009) 125108.
[44] X.Q. Chen, H. Niu, D. Li, Y. Li, Intermetallics 19 (2011) 1275–1281.
[45] T. Petit, P.L. Dulong, Ann. Chim. Phys. 10 (1819) 395.